Available online at www.sciencedirect.com
SCIENCE DIRECT
Journal of Molecular Catalysis A: Chemical 248 (2006) 175–180
JOURNAL OF MOLECULAR CATALYSIS A: CHEMICAL
www.elsevier.com/locate/molcata

Sodium-hypophosphite as a novel reducing agent in the preparation and characterization of silver/silica gel catalysts

Maged Samir Ghattas *

Catalysis Department, Petroleum Refining Division, Egyptian Petroleum Research Institute (EPRI), Nasr City, P.O. Box 11727, Cairo, Egypt

Received 7 May 2005; received in revised form 1 December 2005; accepted 13 December 2005
Available online 30 January 2006

Abstract

New catalysts with different loading 2, 5, 8 and 11 (wt.%) silver on silica gel were prepared by chemical reduction method using a sodium-hypophosphite as a novel reducing agent. The catalytic activity was studied through the dehydrogenation of ethanol in a micro catalytic pulse system at 300–450 °C and at hydrogen flow rate 50 mL/min. The structural changes that accompanying the catalysts preparation were detected by X-ray diffraction, differential scanning calorimetry and infrared techniques. Results show that ethanol dehydrogenation was mainly dependent on the silver content and metal-support interaction. In other words, catalyst sample containing 8% Ag was found the most active and selective for acetaldehyde formation and that contain 11% Ag is rich with silver silicate in certain mode. A texture property of the prepared catalysts was investigated.
© 2005 Elsevier B.V. All rights reserved.

Keywords: Silver catalysts; Ethanol dehydrogenation; Physical properties; Chemical reduction method and sodium-hypophosphite

1. Introduction

In modern industry both the metallic and supported silver-based catalysts are widely used in different purposes. One of these is the removal of NO_x in lean burning exhaust gas using silver ion exchanged zeolite and Ag/Al_2O_3 [1–3].

In recent years, various silica or silica-alumina silver catalysts are used for high catalytic activity and selectivity in the oxidative dehydrogenation of methanol to formaldehyde [4–6,7].

The formaldehyde yield from catalytic oxidation of methanol on Ag/TiO_2–SiO_2 catalysts prepared by *chemical reduction* was ∼13% higher than that of the industrial pumice-supported silver catalyst [8].

The family of Ag/SiO_2 catalysts was thoroughly reduced at 500 °C after calcination step (thermal decomposition of silver nitrate to oxide at 400 °C [9]) then handled carefully in ultra high vacuum system to prevent any exposure to air. This procedure gave metallic silver particles with a range of dispersion from 0.04 to 0.32, thus providing average crystallite sizes between 4 and 31 nm [10].

Silver containing H-ZSM-5 [11,12] and zirconia supported Ag catalysts [13] have high activity for aromatization and deep oxidation of lower alkane. Loading of Ag^+ ions greatly enhances the dehydrogenation of alkane while suppressing the C–C bond cleavage.

Fundamental knowledge of catalytic oxidation mechanisms can be valuable for developing effective methods for using catalysts to control air pollution. Catalytic incinerations of volatile organic compounds like methanol, ethanol, formic acid and acetic acid on Ag/Al_2O_3 catalyst is preferred over thermal incineration for several reasons [14]. Thermal incinerator operates at higher temperatures (700–1200 °C) than catalytic unite (400–500 °C).

The aim of the present study is to investigate the structural features and catalytic activity of some silver/silica gel catalysts prepared by chemical reduction method.

2. Experimental

2.1. Treatment of silica gel support

High purity silica gel support, from Institute Francias de Petrole was refluxed with conc. HCl solution for 45 min and washed several times with distilled water until free from chloride ions.

* Tel.: +2 12 417 3368; fax: +2 2 572 4559
E-mail address: msg_epri@yahoo.com.

1381-1169/$ – see front matter © 2005 Elsevier B.V. All rights reserved.
doi:10.1016/j.molcata.2005.12.014

After washing the sample was dried at 110 °C and calcined at 350 °C in a stream of air for 4 h.

2.2. Catalyst preparation

1. Dissolve the corresponding weight of $AgNO_3$ salt equivalent to 2, 5, 8 and 11% silver metal in distilled water, *solution (A)*.
2. Add dilute ammonia solution to solution (A) until the initial black precipitate redissolves, then add a slight excess of dilute ammonia; *solution (B)*.
3. Add *sodium-hypophosphite (NaH_2PO_2)* to solution (B) in the molar ratio of 1:1.2 with respect to the amount of $AgNO_3$ salt present in solution (A); *solution (C)*.
4. Add solution (C) to slurry of the treated silica gel support *(D)*.
5. Boil the contents of (D) for few minutes, filter and wash with distilled water until free from other components {support + amm. $AgNo_3 + Na_2H_2PO_2 \xrightarrow{\Delta} Ag$}.

2.3. Apparatus and technique

XRD patterns of the investigated samples were recorded using the powder diffraction pattern technique with 2θ ranging between 4° and 90°, with the aid of XD-D1 Shimadzu X-ray diffractometer. The sample was analyzed using Ni filter and Cu Kα radiation at 40 kV and 30 mA. The average crystallite size of silver metal was calculated from Scherrer equation ($D = K\lambda/B_{1/2}\cos\theta$, where, K is crystalline shape factor = 0.9, $\lambda = 1.52$ Å, $B_{1/2}$ is the half width of the diffraction peak and $\cos\theta$ is the Bragg's angle at which the metal appear.

Thermal analysis (DSC) experiments for silica gel support and all prepared catalysts were carried out using Shimadzu thermal analyzer instrument (DSC-50), Japan.

FT-IR spectra of the dried samples were recorded using the KBr disk technique in the range 400–1300 cm^{-1} using a FT-IR Mattson infinity series, USA.

Surface areas were recorded on micromeritics ASAP 2010 at −196 °C using N_2 gas. *Pore size distribution and pore volume* were calculated by BJH method from desorption and adsorption branch of hysteresis loop, respectively). Also *V_l–t plots* were investigated. These were carried out in the catalysis and surface chemistry Laboratory in Faculty of Engineering, Seoul Nat'l University, Seoul, S. Korea.

The conversion of ethanol (in presence of H_2 as carrier gas) was investigated in a pulse system. Ethanol was injected in micro quantities (2 μL) into a micro quartz reactor containing 0.5 g.of the tested samples. The catalyst bed was supported in place on fine quartz wool and an inert glass placed at the top of this bed to ensure good mixing of the reactants. The reactor effluent was passed through a chromatographic column for separation and determination using flame ionization detector. The column used was 200 cm length and 0.3 cm diameter, packed with acid washed chromosorb AW (80–100 mesh size) from Merck, loaded with 15% by weight squalane (Merck). The reactions were carried out under atmospheric pressure and temperature range 250–450 °C. The hydrogen flow rate was kept constant at 50 mL per minute. Prior to catalytic activity test, the catalyst samples were heated in flowing H_2 up to 450 °C with a heating rate of 100 °C/h and kept for 2 h at 450 °C for their activation. Few doses of ethanol were injected first to reach steady state of the activity. The chromatographic column temperature was adjusted and controlled at 60 °C. Computerized data acquisition system was used for integrating and recording the effluent yield.

3. Results and discussion

3.1. X-ray diffraction

The XRD patterns of the Ag/silica gel catalysts are shown in Fig. 1. Distinct XRD patterns attributable to crystallized silver metal at d spacing = 2.36, 2.04, 1.44 and 1.22 Å were identified as those from the crystal faces of Ag (1 1 1), (2 0 0), (2 2 0) and (3 1 1), respectively. As silver loading increases the sharpness of the peak corresponding to the crystal face (1 1 1) increases. The average crystallite size of silver metal (1 1 1) was calculated and found to increase as the silver content increases. This means that, as silver % increase, both particle size and particle crystallinity also increase. The average particle size of the samples containing 5, 8 and 11% Ag (40.5, 41.5 and 43.4 Å, respectively) are almost the same compared to the sample containing 2% Ag (29.8 Å).

The absence of silver oxide phases may be explained as follows: during preparation of the catalysts, the silver nitrate precursor is converted to silver metal by chemical reduction in solution rather than by thermal decomposition of silver nitrate in air to silver oxide followed by reduction to silver metal in hydrogen atmosphere at higher temperature for long time. This results in the formation of silver metal in well crystalline form especially samples contain 5, 8 and 11% Ag. In the sample

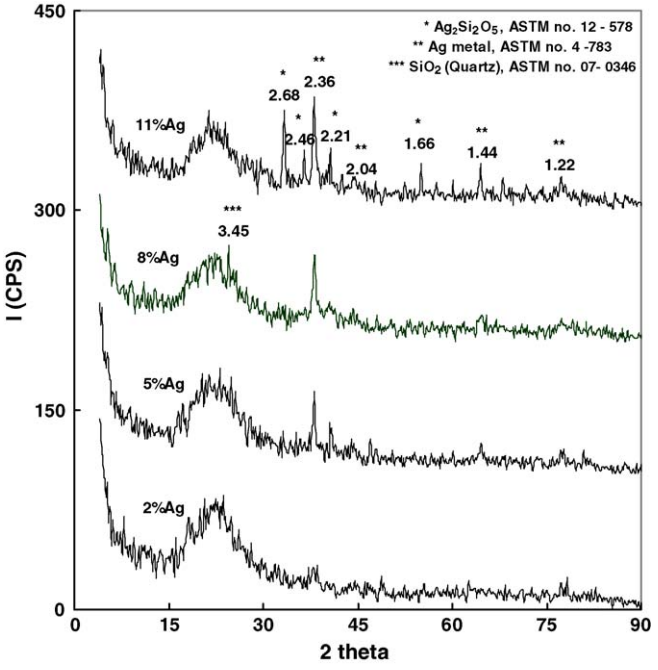

Fig. 1. XRD for Ag/silica gel catalysts with different silver loading.

containing 2% Ag, silver metal peaks are not clearly detected most probably due to its presence in a highly dispersed state.

In Fig. 1 a silver silicate ($Ag_2Si_2O_5$) phase with d spacing = 2.68, 2.46, 2.21 and 1.66 Å was detected. This phase is predominantly present in the catalyst sample containing 11% Ag. The appearance of this phase is due to the interaction of silver ion with silica gel support during preparation of the catalyst. Also this phase was observed in the sample containing 5% Ag.

For the sample containing 8% Ag, a Quartz phase (SiO_2, at *d* spacing = 3.45 Å) was detected and the expected silver silicate phase was absent. This behavior was may be explained on the basis that the silver species act as modifying agent (i.e. seems to have some catalyzing effect) on the silica structure (Si–O–Si) leads to increase or decrease of silica crystallinity according to critical silver concentration. This means that 8% Ag is the suitable concentration to form of quartz phase. Similar observation was noticed in the current research (8% Ni/alumosilicate catalyst) running in our laboratory.

3.2. Textural characteristics of the investigated catalyst sample

It is clear that all isotherms (Fig. 2B) belong to type II of Brunauer and Emmett's classification, exhibiting closed hysteresis loop. The shapes of hysteresis loops of silica and of silver-supported silica are characteristic of mixed pore systems

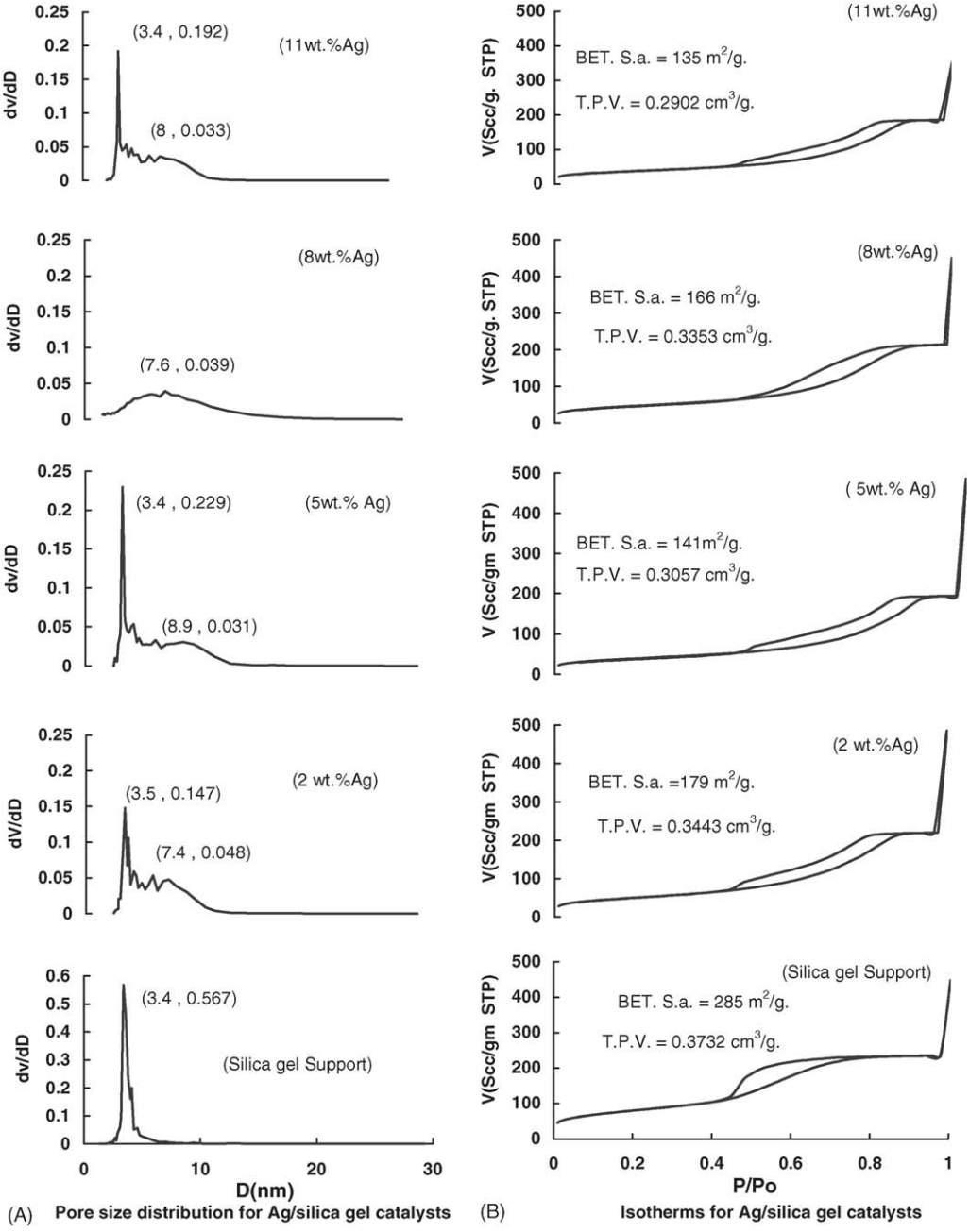

Fig. 2. Textural properties of investigated Ag/silica gel catalysts. (A) Pore size distribution for Ag/silica gel catalysts. (B) Isotherm for Ag/silica gel catalysts.

Table 1
Characteristic adsorption data of investigated catalyst samples

	S_{BET}[a] (m^2/g)	S_t[b] (m^2/g)	V_p[c] (cm^3/g)
Silica gel	285	290	0.3732
2% Ag	179	182	0.3443
5% Ag	141	143	0.3057
8% Ag	166	163	0.3353
11% Ag	135	132	0.2902

[a] Surface area (S_{BET}) estimated from BET equation.
[b] Surface area (S_t) calculated from V_l–t plots.
[c] Total pore volume (V_p) estimated from the saturation value of the adsorption branch of hysteresis loop.

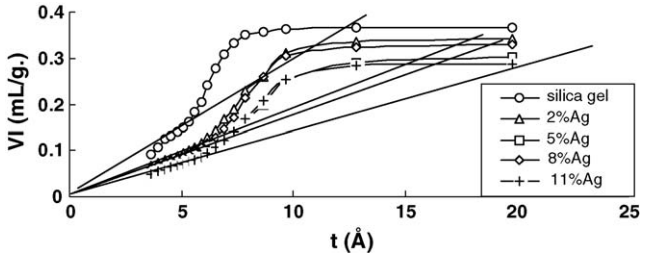

Fig. 3. V_l–t plots for silver/silica gel catalysts.

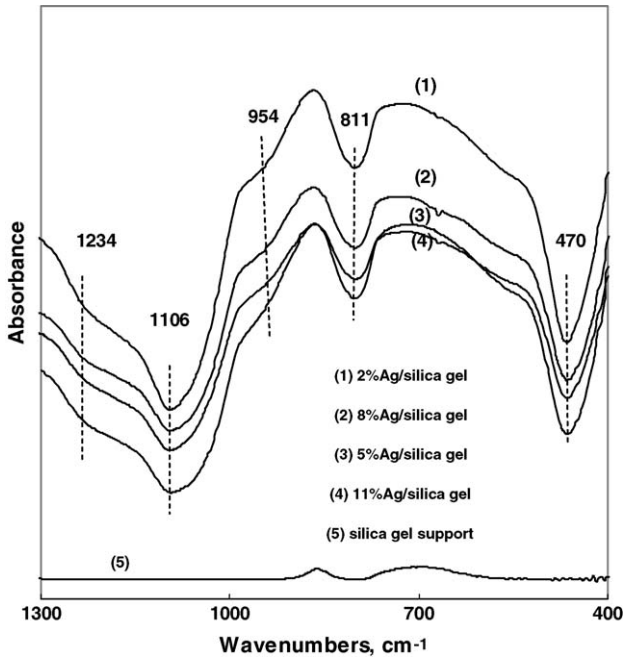

Fig. 4. FT-IR for Ag/silica gel catalysts with different silver loading.

(H3-type). The closure pressures of the hysteresis loops are almost the same, lying in the low-pressure region, viz., ca. 0.42–0.48 P/P_0.

A marked decrease in surface area (S_{BET} and S_t), Table 1 and Fig. 2B, is revealed upon loading with silver metal up to 5% Ag accompanied with a parallel decrease in pore volume. This can be linked with the penetration process especially in the micropores developing more area from mesopores.

For catalyst sample of 8% Ag, some increase in area (166 m^2/g) occurred with parallel increase in pore volume (0.3353 cm^3/g). This may be related to the appearance of some modified pore system (pore widening), Fig. 2A, which is accompanied by the crystallization of some silica gel to quartz.

Further increase in Ag metal content (11% Ag) causes much decrease in both surface areas (135 m^2/g) and pore volume (0.2902 cm^3/g). This may be due to the formation of more silver particles with larger average particle size (43.4 Å). Such particles occupy and block the adsorption sites of the silica gel support together with the formation of silver silicate phase as shown in XRD results.

The V_l–t plots (Fig. 3) were constructed for the catalysts under investigation, where V_l is the volume of N_2 adsorbed (mL g^{-1}) and t is the statistical thickness (Å). From the slope of the straight line obtained passing through the origin, the specific area, S_t (m^2 g^{-1}) was calculated according to $S_t = 10^4 \times (V_l/t)$.

The reasonable agreement between S_{BET} and S_t is the main criterion for the correct choice of the t-curve used in the analysis. The upward deviation from linearity is caused by capillary condensation in mesopores. The downward deviation is due to presence of micropores.

For pure silica support (Fig. 3), an upward deviation is observed, commencing at $t \sim 5$ Å, indicating the predominant existence of mesopores. This deviation does not continue but reverts back at $t \sim 12.8$ Å. Here, mixed pore system is favored. However upon supporting Ag with increasing % loading, the V_l–t plots show increased mesoporosity as the slope of the upward deviation exhibit gradual increase, yet t, values at which the deviation commences remains almost the same ($t \sim 5.5$ Å). Moreover, these plots revert back at increasing t-values, namely, ~18, 18.8 Å for 2 and 8% Ag, respectively. This seems to indicate that the increase in the mesoporous fraction takes place at the expense of the microporous fraction of silica. For both samples containing 5 and 11% Ag, mesoporosity is predominant, some new pore system seems to be created as the continous upward deviation reverts back at much higher t-values, namely, at t ~20 Å.

Table 2
Differential scanning calorimetry (DSC) results

Peak event	Silica gel	2% Ag		5% Ag		8% Ag		11% Ag	
	Endo	Endo	Endo	Endo	Exo	Endo	Endo	Endo	Exo
T_{max} (°C)	129.3	66.91	165.8	59.2	322.3	58.6	384.7	53.4	315.3
Peak hight (mW)	6.1	2.09	0.126	1.17	0.148	1.18	0.043	1.38	0.153
Heat (cal)	4.26	0.15	0.0036	0.0072	0.0053	0.067	0.0015	0.086	0.0053

3.3. Differential scanning calorimetry (DSC)

Pure silica gel (Table 2) shows one endothermic peak at $T_{max} = 129.3\,^{\circ}C$ which is attributed to dehydration of physisorbed water. With increase in silver loading (2–11% Ag), T_{max} corresponding to an endothermic peak decrease much from 66.91 to 53.4 °C, respectively.

According to DSC results (Table 2), exothermic peaks appear at 322.3 and 315.3 °C for samples containing 5 and 11% Ag, respectively, which reflects the formation and recrystallization of a new phase (silver silicate). The same heat value was liberated (0.0053 kcal) in the both samples at both exothermic events showing that the phase formed (silver silicate) in both samples is the same.

The appearance of an endothermic peak at 384.7 °C in the DSC results of the sample containing 8% Ag is attributed to the dehydroxylation of the OH group from silica gel accompanied by crystallization of Quartz.

3.4. FT-IR spectroscopy

The band at 954 cm^{-1} was assigned to the stretching vibration of Si–O of silanol group. The IR spectra of silver/silica gel catalysts are shown in Fig. 4. The bands between 900 and 460 cm^{-1} are associated with the symmetric stretching vibration of Si–O–Si bridges. The more intense and sharp bands at 811 and 470 cm^{-1} present are characteristic to symmetric stretching of Si–O–Si links due to the motion of Si atoms. The intensity of this band is affected by change of silver metal content.

The band at 1106 cm^{-1} is attributed to asymmetric stretching of Si–O–Si links. The broadness of this band increases by increasing the silver content due to the crowdness of Ag metal around Si–O–Si links, so it restrict the motion of asymmetric stretching in the $Ag_2Si_2O_5$ phase especially for samples containing 5 and 11% Ag.

The shoulder at 1234 cm^{-1} is due to stretching Si–O vibration. The latter one and the band at 811 cm^{-1} are classified as external linkage-sensitive.

3.5. Catalytic conversion of ethanol

Fig. 5A shows the catalytic conversion of ethanol over silica gel support, ethylene and diethylether are the products of ethanol dehydration.

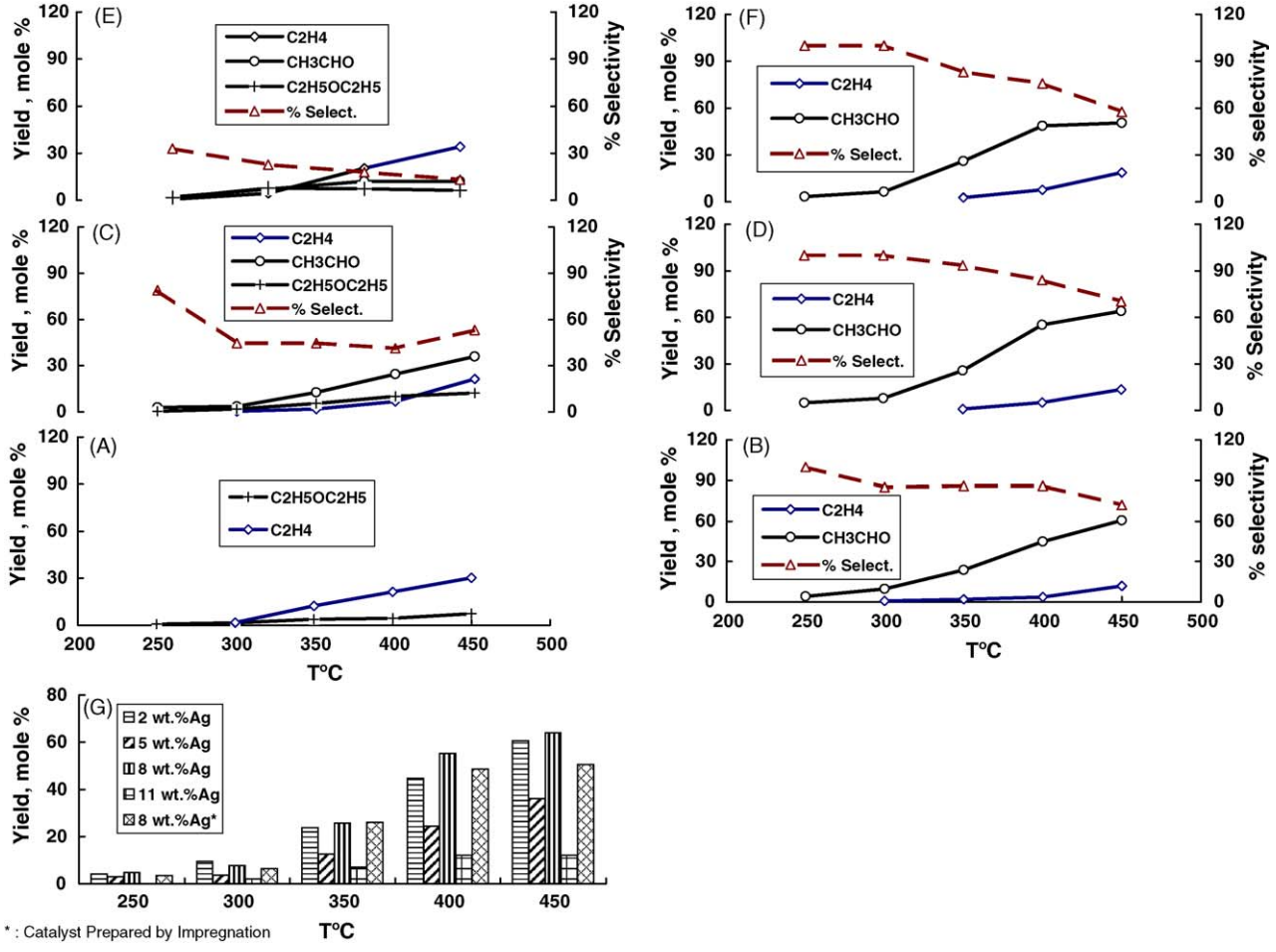

Fig. 5. Catalytic conversion of ethanol over: (A) silica gel support, (B) 2 wt.% Ag/silica gel, (C) 5 wt.% Ag/silica gel, (D) 8 wt.% Ag/silica gel, (E) 11 wt.% Ag/silica gel, all these catalysts prepared by chemical reduction method, (F) 8 wt.% Ag/silica gel prepared by impregnation methode and (G) histograme for acetaldehyde production over silver/silica gel catalysts with different silver loading.

As silver loading increases, ethylene yield decreases up to 8% Ag (Fig. 5D) with minimum yield ~13.5 mol% at reaction temperature 450 °C.

Another product viz. acetaldehyde (selective product) is formed from dehydrogenation of ethanol on the silver/silica gel catalysts. The acetaldehyde formation increased as reaction temperature increased for all catalyst samples.

% Selectivity of acetaldehyde for both samples containing 2 and 8% Ag (Fig. 5B and D, respectively) is higher than other samples 5 and 11% Ag (Fig. 5C and E, respectively). This attributed to their higher surface area (179 and 166 m^2/g, respectively) also to absence of silver silicate species, which is formed in other samples (5 and 11% Ag).

The formation of silicate species causes roughness of the silica surface, thus reducing the pore opening of the support and consequently leads to diminished surface area. The same behavior was shown in the formation of nickel silicate in the Ni/SiO_2 catalysts [15]. Also the decrease in acetaldehyde formation in both samples 5 and 11% Ag is due to the presence of silver silicate species causing decrease of the dehydrogenation rate of ethanol to certain extent.

Eight percent Ag/silica gel catalyst (Fig. 5D) prepared by chemical reduction method gave higher activity and selectivity for acetaldehyde formation rather than the sample prepared by impregnation technique (Fig. 5F). This may be attributed to the silver metal particles formed suffer from increasing the temperature during the preparation (decomposition of supported silver nitrate and reduction of supported silver oxide to supported silver metal). This leads to some extent of particles sintering and decrease of degree of dispersion.

Samples containing 2% Ag and 8% Ag gave high acetaldehyde formation as shown in Fig. 5G.

4. Conclusions

Chemical reduction method is more economically for preparation of supported silver catalysts rather than other preparation methods as impregnation and precipitation methods. Silver supported catalysts are formed in few minutes at a relatively lower temperature (110 °C), meanwhile other methods required long time and high temperature to convert the precursor to metal oxide in presence of air followed by to metal in presence of reducing atmosphere.

Two and 8% silver catalysts prepared by chemical reduction method are good selective and active catalysts for ethanol dehydrogenation to acetaldehyde rather than 5 and 11% silver/silica gel. This being due to the latter samples contain new phase (silver silicate) beside silver metal. This phase is formed as a result of silver–silica gel interaction, which becomes predominant in higher silver containing sample (11% Ag).

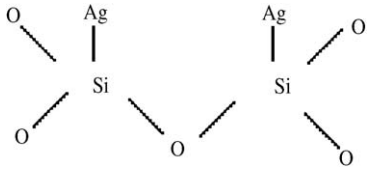

Fig. 6. Silver silicate phase structure.

According to XRD and IR analysis, the structure of silver silicate phase has the form shown in Fig. 6.

The presence of this phase leads to diminishing the surface area and pore volume of 5 and 11% Ag/silica gel catalysts and consequently reduce the catalytic activity of the catalyst.

Thus the catalyst sample containing 2% Ag is recommended for this reaction. It contains lowest silver percent, no silver-silica gel interaction was observed, has high surface area and silver particles seems to be in a highly dispersed state with smaller average particle size.

Acknowledgements

The author gratefully acknowledges assistance by Dr. N.E. Milad (Prof. of Inorganic Chemistry, College of Science, Ain Shams University, Cairo, Egypt) in the catalyst preparation method and for supplying sodium-hypophosphite material.

References

[1] N. Aoyama, K. Yoshida, A. Abe, T. Miyodera, Catal. Lett. 43 (1997) 249.
[2] K.A. Bethke, H.H. Kung, J. Catal. 172 (1997) 93.
[3] M. Haneda, Y. Kintaichi, M. Inaba, H. Hamada, Bull. Chem. Soc. Jpn. 70 (1997) 499.
[4] A.N. Pestryakav, Catal.Today 28 (1996) 239.
[5] Y. Cao, W.-L. Dai, J.-F. Deng, Appl.Catal. 158 (1997) L27.
[6] W.-L. Dai, J.-L. Li, Y. Cao, Q. Liu, J.-F. Deng, Catal. Lett. 64 (2000) 37.
[7] W.-L. Dai, Y. Cao, L.P. Ren, X.L. Yang, J.H. Xu, H.X. Li, H.Y. He, K.N. Fan, J. Catal. 228 (2004) 80–91.
[8] Q. Liu, Y. Cao, W.-L. Dai, J.-F. Deng, Catal. Lett. 55 (1998) 87.
[9] A.N. Pestryakov, Catal. Today 28 (1996) 239.
[10] X. Li, A. Vannice, J. Catal. 151 (1995) 87.
[11] Y. Ono, M. Osako, M. Yamawaki, K. Nakashiro, Zeolites and Microporous Crystals, Elsevier, Tokyo, 1994, pp. 303.
[12] Y. Inoue, K. Nakashiro, Y. Ono, Micropor. Mater. 4 (1995) 379.
[13] L. Kundakovic, M. Flytzani-Stephanopoulos, Appl. Catal. 183 (1999) 35.
[14] E.M. Cordi, J.L. Falconer, Appl. Catal. 151 (1997) 179.
[15] D.J. Suh, J.S. Chung, T. Lim, S.H. Moon, Hwahak Konghok 27 (5) (1989) 620.